

Nanopores with DNA: Strong Electrostatic Interactions in Cellular Dynamics Processes

Motohiko Tanaka¹, and Yitzhak Rabin²

¹*Coordinated Research Center, National Institute for Fusion Science, Toki 509-5292, Japan*

²*Department of Physics, Bar-Ilan University, Ramat-Gan 52900, Israel*

Abstract. Electrostatic interactions play important roles in structure formation of soft condensed matters and biological systems, including the charge inversion phenomena of macroions, the aggregation of like-sign charges colloidal particles, and the DNA translocation through nanopores of cellular membrane. We use molecular dynamics simulations and show how the electrostatic forces control these processes occurring in nanometer to micron scales.

Keywords: Charged colloids, nanopore, DNA, Poisson equation, molecular dynamics

PACS: 87.15.-v, 87.17.-d, 82.20.Wt, 82.39.Pj, 82.70.-y

INTRODUCTION

Electrostatic interactions are not only non-negligible but frequently play important roles in cellular dynamics processes. This is due to the fact that the electrostatic energy between unit charges at room temperature prevails over thermal energy, namely $e^2/\epsilon R > kT$ where e is unit charge, R is the typical ion size, ϵ is dielectric constant and kT is temperature in energy unit. We emphasize that under strong electrostatic forces, two charges of different signs tend to sit closely with each other so that the attraction force becomes larger than the repulsive force in overall electroneutral medium.

We can immediately give two situations where the electrostatic effects become quite prominent at room temperature. One is for the macroions with large charges in water ($\epsilon=80$) containing multivalent salt ions, and the other is for ions in the cell-membrane system. We should note that the dielectric constant of the membrane is by several tens of times less than that of cellular liquid, and for that reason the electrostatic energy is strongly intensified at such interfaces.

A well-known example for the former is the charge inversion phenomena in which a macroion attracts large number of opposite-sign counterions so that the formed aggregate is substantially charged in reverse sign [1-6]. It is also possible that two macroions with like-sign charges aggregate via the mediation of

multivalent counterions. This partly explains the aggregation of (negatively charged) colloidal particles. On the other hand, a good example of the latter is the translocation of DNA through the nanopore of the membrane [7-11]. In the following sections, we first present the aggregation of like-sign charges, and then the behavior of DNA in a nanopore in the membrane.

METHODOLOGY OF MOLECULAR DYNAMICS SIMULATIONS

We use molecular dynamics simulations to study the electrostatic phenomena in liquid medium. The equations of motion for i -th particle are

$$m_i \frac{d\mathbf{v}_i}{dt} = -\nabla(\Phi_p + \Phi_{LJ}), \quad \frac{d\mathbf{x}_i}{dt} = \mathbf{v}_i, \quad (1)$$

where the force on the righthand-side of the first equation is the sum of the Coulombic and the Lennard-Jones forces. The Lennard-Jones potential is always calculated by

$$\Phi_{LJ}(\mathbf{r}_j) = 4\epsilon_{LJ} \sum_j \left[\left(\frac{\sigma}{r_{ij}} \right)^{12} - \left(\frac{\sigma}{r_{ij}} \right)^6 \right], \quad (2)$$

where $r_{ij} = |\mathbf{r}_i - \mathbf{r}_j|$ is the distance between two interacting particles, σ is the sum of radii of these particles, ϵ_{LJ} is the interaction energy. On the other hand, calculation of the Coulombic potential requires some precautions.

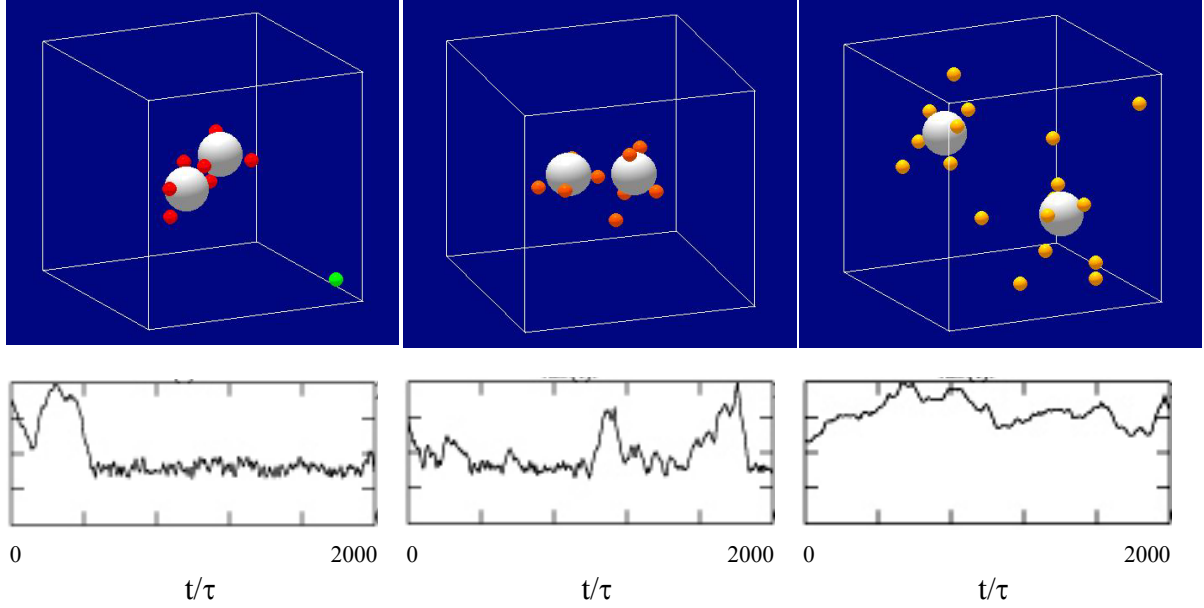


FIGURE 1. Aggregation of like-sign charged macroions (white spheres, $Q=-10e$) occurs through mediation of trivalent counterions (red, left), and divalent counterions (orange, middle), while aggregation does not take place with monovalent counterions (yellow, right). Bottom panels show the temporal variation of the distance between two macroion centers; the ordinate is in the $(0, L/2)$ range and τ is 1ps.

In the system with homogeneous dielectric constant, we can use only direct summation over ions,

$$\Phi_p(\mathbf{r}_i) = \sum_j \frac{q_i q_j}{\epsilon r_{ij}} \quad (3)$$

However, when the dielectric constant $\epsilon(r)$ changes significantly in space, we *must* first solve the Poisson equation

$$\nabla \cdot (\epsilon \nabla \Phi) = -4\pi\rho \quad (4)$$

and make short-range corrections using Eq.(3). This procedure is very important to account for the effects of large spatial inhomogeneity of dielectric constant in the cell-membrane system.

AGGREGATION OF LIKE-SIGN CHARGED IONS IN LIQUID

Aggregation of like-sign macroions is frequently reported in colloidal experiments, and is usually ascribed to van der Waals attraction forces. Here we present other mechanism of the aggregation in which attraction force arises through mediating multivalent counterions.

Figure 1 shows the simulation results of macroions and counterions for three different settings at $e^2/akT=10$ where a is the radius of counterions. Each macroion is negatively charged $-10e$, and counterions

are trivalent $3e$ (red, left), divalent $2e$ (orange, middle) and monovalent e (yellow, right). The whole system is electroneutral and periodic in three directions. Solvent is represented by many neutral particles of $\epsilon=80$. In the left frame, three trivalent counterions are sandwiched by two macroions and they serve to glue the macroions by electrostatic attraction forces against repulsion between macroions. This aggregate is stable in time as shown in the bottom frame, and this process resembles covalent bonding of two nuclei by sharing electrons.

Monovalent counterions are not capable of binding two macroions, as depicted on the right frames. A part of counterions condense on randomly positioned macroions. Divalent counterions, orange spheres in the middle frame, attract macroions but aggregation is not firm enough.

The force balance between macroions is estimated as follows. For the case of trivalent counterions, the attraction between the macroion and counterions and the repulsion between the macroions are calculated to be $\Phi \sim 3ZeQ/R + Q^2/2R = (3Ze+Q/2)Q/R = 4eQ/R < 0$, which is attractive; Z is the valence of the counterion, Q and R are the charge and radius of the macroion. For the divalent counterions, $\Phi \sim eQ/R$ and is slightly attractive, while for the monovalent counterions the potential is estimated to be repulsive when the macroions make close contact $\Phi \sim -2eQ/R > 0$. Actually, the number of condensed counterions should be determined theoretically. The simple estimation here is in agreement with the results of Fig.1.

NANOPORES WITH DNA

The DNA that carries genetic information in living cells is a charged polymer having a unit charge at the phosphate group in every few Angstrom interval along its thread. When the DNA migrates between cellular liquid of the dielectric constant $\epsilon_w = 80$ through a pore embedded in the cell membrane, the pore both geometrically and electrostatically affects the DNA and ion distributions [7-11]. The membrane is characterized by the low dielectric constant $\epsilon_m = 2$, thus the electrostatic energy

$$W_E = \epsilon E^2 / 2 = D^2 / 2\epsilon \quad (5)$$

is enhanced roughly by ϵ_w / ϵ_m times ($\gg 1$) since the electric displacement $D = \epsilon E$ is continuous. In this respect, the electrostatic interactions are expected to be very important in the life processes.

In order to study the behavior of DNA and ions in the nano-sized pore, we have performed molecular dynamics simulations [11]. We take a rectangular box separated into upper and lower compartments by an inserted membrane at the middle. The membrane is pierced by a cylindrical pore extending along the vertical axis, where the pore and compartments are filled with cellular liquid of large dielectric constant ϵ_w . Salt ions KCl of 1M and (neutral) solvent particles that emulate cellular liquid are put in this volume. Because of the electrostatic interactions and large inhomogeneity of the dielectric constant, the Poisson equation Eq.(4) *must* be solved for charge density $\rho(r)$ and the dielectric constant $\epsilon(r)$ on top of the short-range

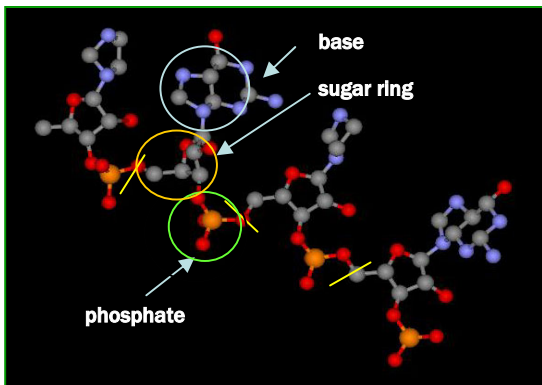


FIGURE 2. Molecular sketch of a single-stranded DNA and our model DNA consisting of three kind of connected monomers that represent the negatively charged phosphate group, a sugar ring and a side chain base.

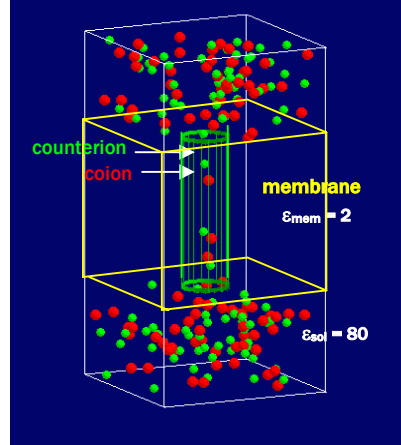


FIGURE 3. A nano-sized pore without DNA inside. The yellow rectangular region corresponds to the membrane of low dielectric constant, and the green cylinder represents the nanopore. Note that K^+ ions (green) and Cl^- ions (red) are forming pairs in the pore.

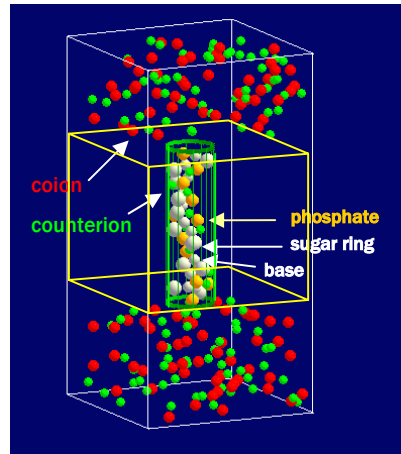


FIGURE 4. A nanopore with a single-stranded DNA inside. Coions (red) are almost completely depleted from the pore, while counterions (green) condense on the DNA and neutralize it. The phosphate group (monomer) is shown by an orange sphere.

Coulombic corrections and Lennard-Jones forces. We adopt the conjugate gradient method to solve Eq.(4) under non-trivial configuration.

We model a single-stranded DNA by connected nucleic acid units, as depicted in Fig.2 where gray, blue, red and orange atoms represent carbon, nitrogen, oxygen and phosphate atoms, respectively (hydrogen atoms are not displayed). Each unit consists of three monomers, one charged group and one neutral monomer on the backbone that correspond to the

TABLE 1. Comparison of average charges, their fluctuations and DNA end-to-end distances for three different nanopores of 7.5Å radius, 50Å length, and dielectric constant $\epsilon=2$ or 80 [11].

	Empty pore $\epsilon=2$	ss-DNA stuffed pore $\epsilon=2$	ss-DNA stuffed pore $\epsilon=80$
Charge of counterions	2.2 ± 1.5	11.5 ± 1.0	11.8 ± 1.2
Charge of coions	2.2 ± 1.6	0.4 ± 0.5	1.7 ± 0.9
DNA charge	--	11.7 ± 0.5	11.8 ± 0.4
Net charge	0.06 ± 0.7	-0.6 ± 0.9	-1.7 ± 1.2
DNA end-to-end distance	--	44Å	42Å

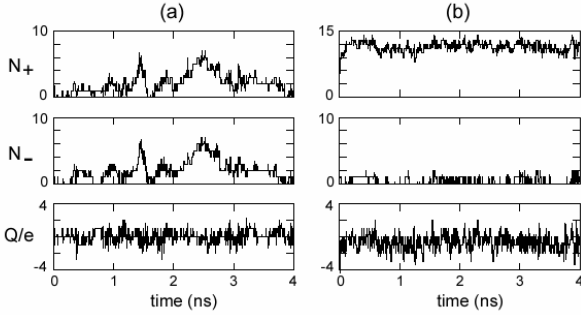


FIGURE 5. (a) The time history of the numbers of counterions N_+ , coions N_- , and the total charges ($Q=e(N_+-N_-)$) contained in the empty pore (no DNA) is shown. (b) The time history in the presence of DNA (with $N_{DNA} \sim 12$) in the pore. The total instantaneous charge contained in the pore is $Q=e(N_+-N_- - N_{DNA})$. In both cases, the dielectric constant is $\epsilon_m=2$.

phosphate group and the sugar ring, respectively, and a base monomer is attached as the side chain.

We have clearly shown on the basis of the simple physical model above [11], that when the DNA is not present in the pore, isolate ions cannot reside inside the pore but only aggregated pairs of counterions and coions can exist in it because of the electrostatic repulsion from the membrane (Fig.3). The charges of counterions and coions fluctuate in time as shown in Fig.5(a) and listed in Table 1, but the net charge in the pore is almost nullified since those fluctuations are synchronized due to intensification of electrostatic energy there.

When the DNA is present in the pore (Fig.4 and Fig.5(b)), the DNA is subject to complete counterion condensation to reduce electrostatic energy (see also Table 1). For the same reason, coions are repelled from the negatively charged DNA and are depleted from the pore. The DNA is elongated in the pore compared with the bulk phase for which the end-to-end distance of DNA is 34Å. This is due to electrostatic repulsion and the geometrical constraint from the membrane and the pore wall.

The effects of the electrostatic interactions are best seen when one compares the actual and artificial cases in Table 1, namely, the membranes having the low $\epsilon_m=2$ and large $\epsilon_m=80$ dielectric constants (the low dielectric constant of the membrane arises from oily nature of the hydrophobic bilayer with hydrophilic heads outside). The DNA is condensed by counterions and charge neutralized while coions are markedly depleted from the pore in the former, but there exist a few coions in the latter case. This clearly proves the important role of the electrostatic interactions in the actual life processes.

We have examined the diffusion process of counterions and coions through the nanopore, and also the pore current when a voltage bias is applied between the top and bottom electrodes. With the DNA present inside the pore, the diffusion rate of counterions, which are the principal carrier of the pore current (coions are depleted), is suppressed roughly by a factor of three compared with that for the DNA-absent pore. This shows the blockade effect of DNA.

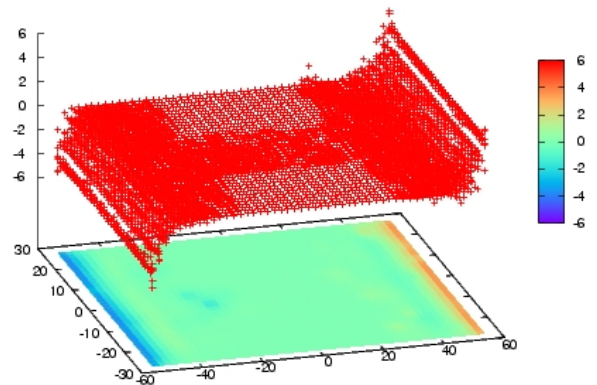


FIGURE 6. The electrostatic potential on the central plane is color mapped, and is also shown in 3D contours; the left and right edges correspond to the bottom and top electrodes, respectively, and the nanopore is the region with potential deviations along the side axis. Large potential drop occurs at the Debye sheath near the electrodes.

The amount of decrease in the free diffusion rate appears to be somewhat less than the decrease in the measured current through the α -hemolysin pore [9].

Figure 6 shows the electrostatic potential on the central plane (cross section) for the voltage-biased simulation, in which the top and bottom electrodes (endplates) are fixed at the voltage $V_{\text{top}} = 5kT$ and $V_{\text{bottom}} = -5kT$, respectively. The voltage-bias between the two electrodes is then $10kT \sim 250mV$. Cations/anions arriving at the electrodes are removed and reinjected in the opposite cells. The potential changes nearly one-dimensionally along the z -axis (the direction from the bottom to top electrodes). It is quite remarkable that a large drop of the electrostatic potential occurs in the vicinity of the electrodes.

The electrostatic potential along the central chord along the z axis is shown in Fig.7 where the potential is plotted in the kT unit. The electrostatic potential profile is approximately the solution of the Poisson-Boltzmann equation. There are Debye sheathes at the electrodes, and the potential changes very gradually in the nanopore. The potential gap between the entrance and exit of the nanopore is about $0.5kT$. It is emphasized that this gap is only 5% of the applied voltage bias between the electrodes, in contrast to the assumption used in [10]. Yet, the measured current through the nanopore in the molecular dynamics simulation is roughly one ion charge in $1ns$, $1e/ns$, which is $150pA$ and agrees with the observed current in the above-quoted experiments [9].

SUMMARY

We have demonstrated in this article using the molecular dynamics simulations that the electrostatic interactions, which are often left out in theoretical studies, play important roles in room-temperature soft condensed matters. These phenomena including colloids and life processes such as DNA, cell and membrane, occur because the electrostatic energy becomes several times that of thermal energy.

We have presented two typical phenomena, (i) the aggregation of like-sign macroions through mediation (glue effect) by multivalent counterions, and (ii) the behavior of DNA and cations/anions in the nanopore. Pore current is controlled by electrostatic effects. The key physics of these processes is the intensification of electrostatic energy in the membrane having low dielectric constant compared to surrounding cellular liquid (salt water). For theoretical studies as shown here, the Poisson equation needs to be solved under spatially inhomogeneous dielectric constant.

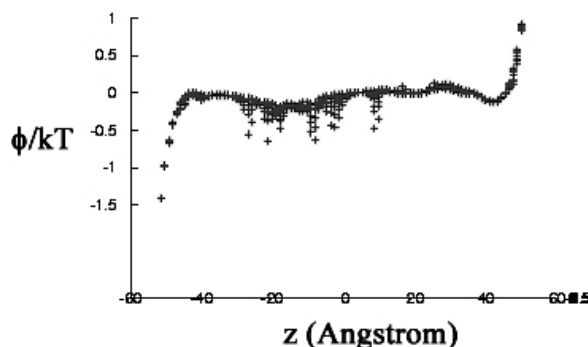


Figure 7. The electrostatic potential between two electrodes (along the z axis) is shown in the kT unit. The central region between $z = -25$ to 25 corresponds to the nanopore. Note the small potential gap $0.5 kT$ across the pore compared to the applied voltage bias $10 kT$ between the electrodes.

ACKNOWLEDGMENTS

The authors acknowledge fruitful discussions with Prof. A. Yu. Grosberg and Prof. B. I. Shklovskii. One of the authors (M.T.) was supported by the Grant-in-Aid No. 16032217 (2003-2005) from the Japan Ministry of Education, Science and Culture. Computations were performed using the computers of the Institute of Molecular Science (Japan) and the in-house PC cluster (Beowulf) machines.

REFERENCES

1. B. I. Shklovskii, *Phys. Rev.*, **E60** (1999) 5802.
2. R. Messina, C. Holm and K. Kremer, *Phys. Rev. Lett.*, **85** (2000) 872.
3. M. Tanaka and A. Grosberg, *J. Chem. Phys.*, **115** (2001) 567.
4. M. Tanaka and A. Grosberg, *Euro. Phys. J.* **E7** (2002), 371.
5. A. Grosberg, *Rev. Mod. Phys.*, **74** (2002) 329.
6. M. Tanaka, *Phys. Rev.*, **E68** (2003) 061501.
7. J. Kasianowicz, E. Brandin, D. Branton, and D. Deamer, *Proc. Natl. Acad. Sci.*, **93** (1996) 13770.
8. M. Akeson, D. Branton, J. Kasianowicz, E. Brandin and D. Deamer, *Biophys. J.*, **77** (1999) 3227
9. A. Meller, L. Nivon and D. Branton, *Phys. Rev. Lett.* **86** (2001) 3435.
10. D. K. Lubensky and D. R. Nelson, *Biophys. J.*, **77** (1999) 1824.
11. Y. Rabin and M. Tanaka, *Phys. Rev. Lett.*, **94** (2005) 148103.